

Model of an unglazed photovoltaic thermal collector based on standard test procedures

Martin Stegmann¹, Erik Bertram¹, Gunter Rockendorf¹, Stefan Janßen²

¹ Institut für Solarenergieforschung Hameln/Emmerthal (ISFH)

Am Ohrberg 1, 31860 Emmerthal (Germany); tel.: 05151/999-645; e-mail: m.stegmann@isfh.de

² janßen energieplanung, Hohenzollernstraße 51, 30161 Hannover (Germany)

1. Introduction

Existing PVT collector models are in general using physical balance and transfer equations, thus they are basing on the design data. Furthermore most of the models are simulating glazed PVT collectors. This paper presents a new model for unglazed liquid cooled PVT collectors that is based on the combination of parameters resulting from conventional thermal and electrical performance measurement data and their characteristic curves, which are obtained in standard test procedures. The thermal performance parameters are taken from a collector test according to EN 12975-2, while for the PV part, the “effective solar cell model” has been chosen, which uses results from a test according to EN 60904-1. Hence, only experimental performance parameters from established test methods are required to describe the complete PVT collector performance. In addition to this characteristic curve modelling, a physical approach is implemented for describing the condensation effects. Furthermore, the model takes the internal heat transfer coefficient between PV cells and fluid into account. This coefficient may be derived from the thermal performance parameters. The model has been transferred into the simulation program TRNSYS and tested against short-term measurements on a test roof and validated against measurements in a 40 m² PVT collector field over the period of one year. The work presented in this paper has been realized within the project “Solar heat supply for buildings with unglazed photovoltaic thermal collectors, borehole heat exchangers and heat pumps”¹.

In the research project heat supply systems for buildings with heat pump and borehole heat exchanger are investigated. In typical systems the borehole heat exchanger temperature decreases within the first years of operation. In consequence, the efficiency of the system is decreasing and more electrical energy is needed to deliver the required heat. To prevent this temperature decrease a solar thermal collector can be used to inject solar thermal heat in the borehole and regenerate the earth temperature. So, the temperature level and the system’s efficiency of the first year of operation are kept stable over the following years (Bertram, 2009). In the system investigated an unglazed PVT collector has been selected, because the needed collector outlet temperature has not to be higher than 30°C. In addition to the improved heat pump efficiency, the PV cells in the used PVT collector are cooled. This increases their electrical efficiency. So, the use of PVT collectors in such systems leads to a double benefit, which reduces the electrical energy demand for the heat pump and increases the electrical yield in comparison to a not cooled PV power plant of identical size.

2. TRNSYS model for unglazed PVT collector

Most of the existing models need design data for parameterization, which normally are unknown for the model operator. In the research project a simulation model was needed, that uses data from standard performance tests and includes the effects of air speed, infrared radiation, thermal collector capacity and condensation on collector surface. As no appropriate model has been available to describe the dynamic behaviour of an unglazed PVT collector in the necessary accuracy, a new model had to be developed and implemented in TRNSYS.

2.1. Model concept

The core of the model concept is the combination of two characteristic performance models for an unglazed thermal collector and a standard PV module. The thermal model is described by the measured performance

¹ The project “Solare Gebäude-Wärmeversorgung mit unverglasten photovoltaisch-thermischen Kollektoren, Erdsonden und Wärmepumpen für 100% Deckungsanteil (acronym BiSolar-WP)“, FKZ 0325952, in cooperation with the company GEFGA, is funded by the German Federal Ministry for the Environment, Nature Conservation and Nuclear Safety (BMU) based on a decision of the German Federal Parliament. The content of this publication is in the responsibility of the authors.

characteristic according to EN 12975-2 and the electrical model is described by the empirical “effective solar cell model” (Wagner, 2006), which only requires standard performance test data of PV modules. Accordingly, only parameters from established performance tests and manufacture standard data sheets are needed for the dynamic calculation of the thermal heat flow rate and the electrical power. Both characteristics are interconnected via the incoming energy path and the PV cell temperature.

2.2. Thermal collector model

The thermal collector model for unglazed solar thermal collectors is based on the characteristic performance model with a transient energy balance. The characteristic curve is described in EN 12975-2. The model takes the influence of solar radiation (beam and diffuse), air speed, fluid, ambient and sky temperature into account. It also regards the reduction of radiation by the incident angle modifier for thermal absorbers, the dynamic behaviour and the effects of condensation on the collector surface. For the calculation of condensation the characteristic curve model was extended by a physical approach.

2.3. Electrical model (PV module)

For the extension of the thermal model to a PVT collector model the particularly suitable characteristic curve model “effective solar cell model” was used, which is an empirical mathematical function valid for standard PV modules. Its inaccuracy is reported to be less than 1% (Wagner, 2006). It calculates the electrical power of a standard PV module by using the characteristics from the manufacturer’s data sheet, the incident radiation and the cell temperature. It therefore may be easily parameterized. The electrical power is calculated at the maximum power point (MPP) at the DC side.

2.4. Combination of the two characteristic performance models

The PVT collector model is composed by the combination of the models for the thermal and the electrical energy path. Fig. 2.1 shows the principle of the PVT collector model.

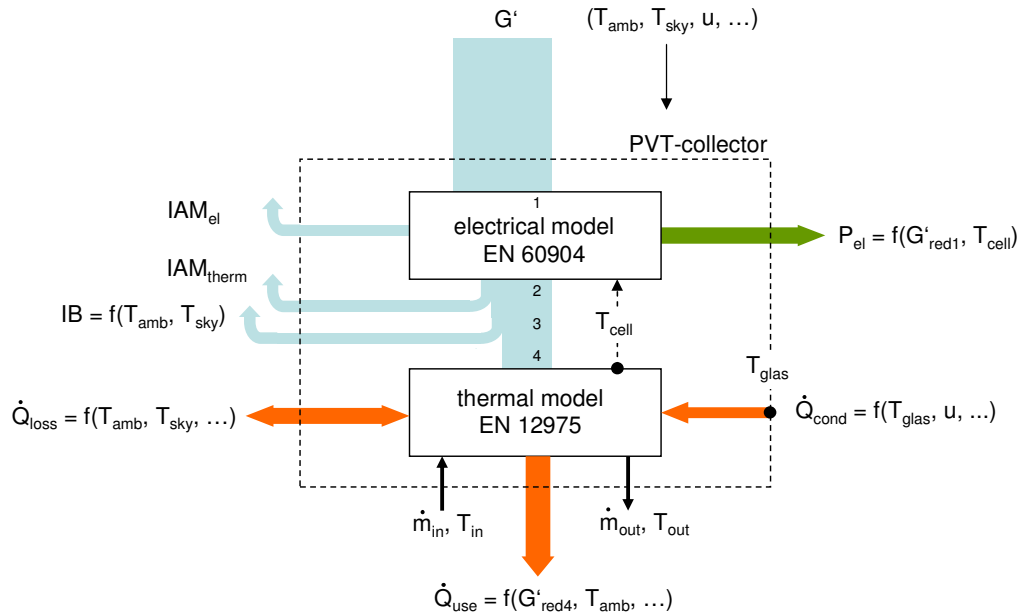


Fig. 2.1: Combination of the two characteristic curve models for thermal collector and PV module to a PVT collector model

2.5. Radiation splitting

The incident radiation on collector surface G' is reduced by the incident angle modifier IAM_{el} for the electrical PV module (eq. 1). Therefore the transversal and the longitudinal incident angle correction factors for beam radiation (eq. 2) and the incident angle correction factor for diffuse radiation is taking into account. From the remaining radiation G'_{red1} a fraction of the IAM- modified radiation is converted into electrical power P_{el} . For the conversion into heat the available radiation G'_{red2} is the difference between the incoming radiation G' and the electrical power P_{el} (eq. 3). Corresponding to the electrical IAM_{el} reduction, the radiation G'_{red2} is reduced by the incident angle modifier IAM_{therm} for the thermal part of the model (eq. 1

and eq. 2). Afterwards the radiation G'_{red3} is reduced by the infrared radiation balance IB to take into account the long wave radiation emitted to the sky (eq. 4). So for the conversion into heat the net radiation G'_{red4} is remaining (fig. 2.1).

$$G'_{red1} = G' \cdot \left[k_{\Theta,beam,eff,PV}(\Theta) \cdot \left(1 - \frac{G'_{dif}}{G'} \right) + k_{dif,PV} \cdot \frac{G'_{dif}}{G'} \right] \quad (\text{eq. 1})$$

$$k_{\Theta,beam,eff,PV}(\Theta) = k_{\Theta,beam,t,PV}(\Theta_t) \cdot k_{\Theta,beam,l,PV}(\Theta_l) \quad (\text{eq. 2})$$

$$G'_{red2} = \left(G' - \frac{P_{PV}}{A_{PVT}} \right) \quad (\text{eq. 3})$$

$$G'_{red4} = G'_{red3} + \frac{\varepsilon}{\alpha} \cdot \left(G'_{IR} - \sigma \cdot (T_{amb} + 273.15K)^4 \right) \quad (\text{eq. 4})$$

2.6. Heat flow rate

The conversion of the radiation G'_{red4} into the useful heat flow rate and the heat losses to the ambient air is calculated according to the quasi-dynamic model of EN 12975-2. It consists in a transient energy balance (eq. 5), that includes the conversion of incoming radiation G'_{red4} with heat losses against the ambient, the collector heat flow rate \dot{q}_{use} and the thermal collector capacity c_{eff} . The model is completed by the term \dot{q}_{cond} , which represents the heat flow rate caused by condensation effects.

$$c_{eff} \frac{dT_m}{dt} = G'_{red4} \cdot \eta_0 \cdot (1 - b_u \cdot u) - (b_1 + b_2 \cdot u) \cdot (T_m - T_{amb}) + \dot{q}_{cond} - \dot{q}_{use} \quad (\text{eq. 5})$$

2.7. Electrical power

The electrical power of the PVT collector is calculated with the relative efficiency factor η_{rel} , which is the ratio of present efficiency to the efficiency at standard test conditions η_{STC} of the used PV module (eq. 6). The relative efficiency considers the cell temperature, the amount of solar radiation and the PV module properties (eq. 7). To describe the properties of the used PV module, the following auxiliary parameters are needed. The imaginary photovoltaic resistance R_{PV} and the physically variable temperature voltage U_T of the “one diode model” (Wagner, 2006).

$$P_{PV} = \eta_{STC} \cdot \eta_{rel} \cdot G'_{red1} \cdot A_{PVT} \quad (\text{eq. 6})$$

$$\eta_{rel} = \left(1 + c_T \cdot (T_{cell} - T_{STC}) \right) \cdot \left(1 + \frac{U_{T,STC}}{U_{MPP,STC}} \cdot \ln \left(\frac{G'_{red1}}{G'_{STC}} \right) - \frac{R_{PV,STC} \cdot I_{MPP,STC}}{U_{MPP,STC}} \cdot \left(\frac{G'_{red1}}{G'_{STC}} - 1 \right) \right) \quad (\text{eq. 7})$$

2.8. Cell temperature

To calculate the electrical power the cell temperature is needed. Starting from the mean fluid temperature T_m the cell temperature T_{cell} is calculated with the heat flow rate \dot{q}_{use} and the internal heat transfer coefficient u_{int} . This is valid under the assumption, that the solar cell is the location, where most of the heat is produced.

$$T_{cell} = \frac{\dot{q}_{use}}{u_{int}} + T_m \quad (\text{eq. 8})$$

2.9. Condensation effects

Unglazed PVT collectors can collect useful heat by condensation. Condensation on the outer surface of the PVT collector appears when the temperature on the PVT collector surface is below the dew point temperature T_d of the ambient air. This additional condensation heat is transferred to the circulating fluid. To calculate the surface temperature of the PVT collector T_{glass} a physical submodel with the network shown in fig. 2.2 is used. In this submodel the effects of radiation to the sky and convective heat transfer to ambient air is considered. The surface temperature determined according to eq. 15 is only used for the calculation of the condensation heat flow rate (eq. 9). The collector heat flow rate itself is calculated by (eq. 5).

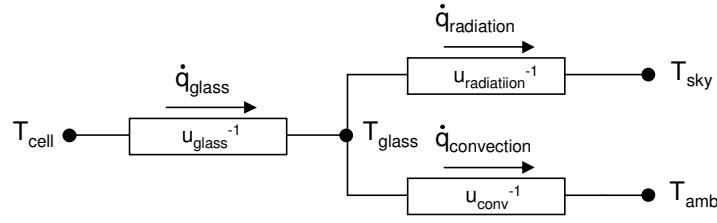


Fig. 2.2: Heat resistance network for the calculation of PVT collector surface temperature (glass)

$$\dot{q}_{cond} = \frac{R_L}{R_D} \frac{\Delta h_v}{p_0 c_L} Le^{m-1} u_{conv} [p_s(T_{glass}) - p_s(T_d)] \quad \text{with } m \sim 1/3 \quad (\text{eq. 9})$$

The convective heat transfer coefficient u_{conv} is calculated by an empirical function (eq. 10). For the radiation to sky the heat transfer coefficient $u_{radiation}$ is given by (eq. 11) with the effective ambient temperature T_{eff} (eq. 12). The view factor F accounts that a collector with a slope β partially sees the sky and partially sees the ground, which is assumed to be at ambient temperature (eq. 13). The heat transfer coefficient of the PVT collector cover u_{cover} is calculated with (eq. 14).

$$u_{conv} = \sqrt[3]{(0,123 \cdot (T_{glass} - T_{amb}) + 2,7)^3 + (2,83 \cdot u + 4,3)^3} \quad (\text{eq. 10})$$

$$u_{radiation} = \sigma \cdot \epsilon_{glass} \cdot (T_{glass}^2 + T_{eff}^2) \cdot (T_{glass} + T_{eff}) \quad (\text{eq. 11})$$

$$T_{eff} = \sqrt[4]{F \cdot T_{sky}^4 + (1 - F) \cdot T_{amb}^4} \quad (\text{eq. 12})$$

$$F = 0.5 \cdot (1 + \cos \beta) \quad (\text{eq. 13})$$

$$u_{cover} = \left(\frac{d_{glass}}{\lambda_{glass}} + \frac{d_{foil}}{\lambda_{foil}} + \dots + \frac{d_n}{\lambda_n} \right)^{-1} \quad (\text{eq. 14})$$

$$T_{glas} = \frac{T_{cell} \cdot u_{cover} + T_{eff} \cdot u_{radiation} + T_{amb} \cdot u_{conv}}{u_{cover} + u_{radiation} + u_{conv}} \quad (\text{eq. 15})$$

3. Determination of internal thermal conductance from thermal measurement

The direct measurement of the internal heat transfer coefficient u_{int} between the absorber (cell) and the fluid is particularly for PVT collectors very difficult. The assembly of sensors directly on the PV cells which form the absorber is hardly possible. Furthermore the determination of the internal heat transfer coefficient is not a part of the EN 12975-2 performance test. But for the calculation of the electrical PV power the PV cell temperature is essential. Hence, a calculation method for u_{int} is proposed by using the data of the thermal performance test and integrated in the TRNSYS model.

The u_{int} value is approximately constant over all operation conditions of the collector. This assumption is valid for constant material data and flow rates, i.e. it may be used, if the relevant temperature and flow rate ranges are kept small. This is the case for unglazed collectors. In particular, the u_{int} value may be regarded as independent from ambient air speed. In contrary to a glazed collector the conversion factor of an unglazed collector is far more a function of the air speed. This air speed dependent conversion factor $\eta_{0,u}$ of the thermal performance is derived from the EN 12975 test (eq. 5, see also (Duffie & Beckman, 2006)) under steady state conditions, at a fluid temperature which equals the ambient temperature (eq. 16). The slope of the thermal performance curve $b_{v,u}$, which represents the collector heat losses, is given by the thermal performance curve (see eq. 5) and may be described with (eq. 17). Furthermore the collector efficiency factor F' as a function of the loss coefficient and with it as a function of air speed is defined by (eq. 18), (Rockendorf, 1995).

$$\eta_{0,u} = \eta_0 \cdot (1 - b_u \cdot u) = F'_u \cdot \alpha \quad (\text{eq. 16})$$

$$b_{v,u} = b_1 + b_2 \cdot u = F'_u \cdot u_{loss,u} \quad (\text{eq. 17})$$

$$F'_u = \frac{u_{int}}{u_{int} + u_{loss,u}} \quad (\text{eq. 18})$$

With (eq. 16) to (eq. 18) the internal heat transfer coefficient can be calculated by (eq. 19).

$$\Rightarrow u_{int} = \frac{F'_u \cdot u_{loss,u}}{1 - F'_u} = \frac{b_{v,u}}{1 - \frac{\eta_{0,u}}{\alpha}} = \frac{\alpha \cdot b_{v,u}}{\alpha - \eta_{0,u}} = \frac{\alpha \cdot (b_1 + b_2 \cdot u)}{\alpha - \eta_0 \cdot (1 - b_u \cdot u)} \quad (\text{eq. 19})$$

This procedure leads to a set of u_{int} values for varying air speed levels. These values should be approximately identical. This requirement may serve as a control algorithm, whether the collector parameters are appropriate.

4. Development and Validation Procedure

The PVT collector model is developed and tested in TRNSYS on test rig measurements and validated on a measurement of a 40 m² PVT collector field in a heat pump system with borehole heat exchanger over the period of one year. For parameterization of the model the thermal parameters are derived from a standardized thermal measurement according to EN 12975-2 in open circuit operation. The electrical parameters are derived from the manufacturer's data sheet for the used PV module. For the incident angle modifier of the electrical side data were taken from a measurement (Balanzategui, 2004) of a standard PV-module. After a plausibility check the same data were taken for the thermal incident angle modifier. The model was supplied with the measured meteorological data as inputs. In the pilot plant the simulation results are compared with daily yields over the period of one year. The test rig measurements are tested in 1 minute yields over a period of 21 hours.

4.1. Quantifying of the validation results

The deviation of thermal yield ΔQ and electrical yield ΔE_{el} is calculated with the formula in (eq. 20). It shows the relative deviation between simulated and measured thermal and electrical yield.

$$\Delta Q = \frac{\sum(Q_{sim} - Q_{meas})}{\sum Q_{meas}} \quad \Delta E_{el} = \frac{\sum(E_{el,sim} - E_{el,meas})}{\sum E_{el,meas}} \quad (\text{eq. 20})$$

In addition to that, the relative square deviation (Hilmer, 1999) for thermal and electrical yield was calculated by (eq. 21). The term \bar{x}_{meas} is the mean value of the measured yield over all intervals of the measured period. For the validation in the pilot plant over the period of one year, the deviation of daily total yields and the mean value of all daily yields over this year were used.

$$\bar{V} = \frac{1}{N} \cdot \sum_{i=1}^N \sqrt{\frac{(x_{sim} - x_{meas})^2}{\bar{x}_{meas}^2}} \quad (\text{eq. 21})$$

4.2. Test rig measurements for plausibility checks

For the test rig plausibility check during the development, the PVT collector was measured with electrical power production by connection to a conventional small power inverter for single PV modules. During the measurements the PVT collector was operated in the point of maximum power. The measured data were recorded in time steps of 30 s. The uncertainty of measurement for thermal yield has been determined to $\pm 2.5\%$ and for the electrical yield within $\pm 0.6\%$, not taking into account the uncertainty of the data logger (which is small) and the failure of the MPP tracker.

In TRNSYS the output was simulated in time steps of 1 minute. For that purpose the collector model was parameterized like the measured PVT collector and the measured data were used as model inputs. For the plausibility check on test rig a time period of 3 measuring days with total 21 hours with dynamic weather

conditions were available. The deviation for thermal yield between simulation and measurement is -3.1% and 12.5% for relative square deviation. Fig. 4.1 shows the results for a time period of 7 h on July 03, 2009.

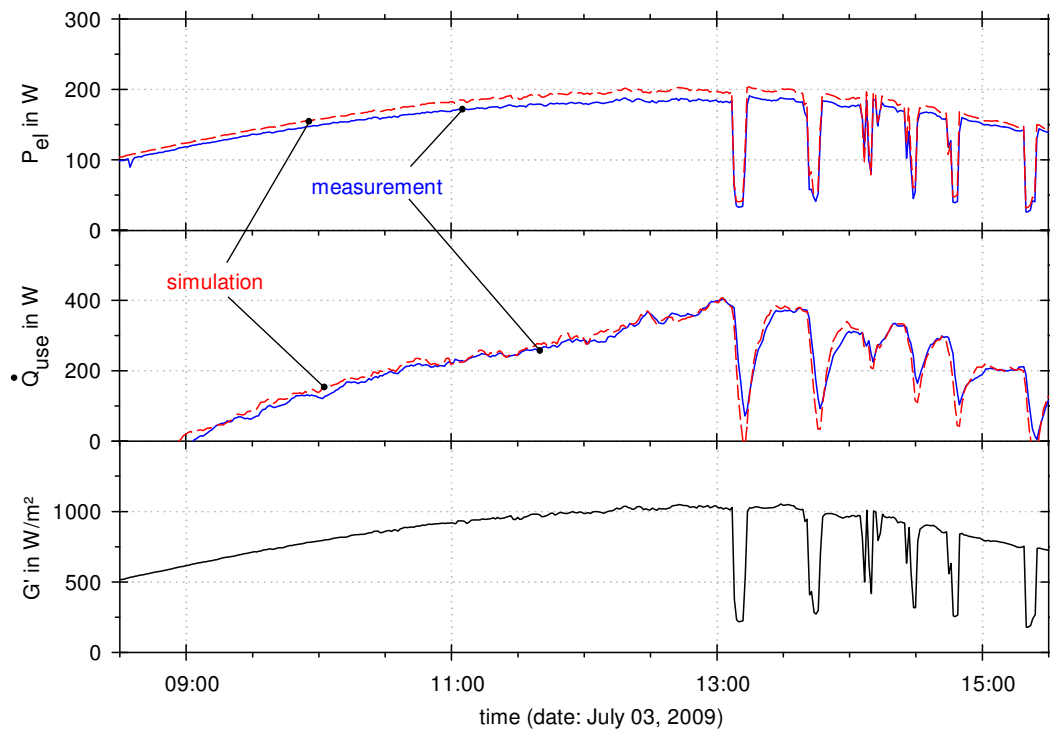


Fig. 4.1: Measured and simulated electrical power and heat flow rate and radiation over a period of 7 hours

According to these results the thermal heat flow rate is reproduced with good accuracy, only with an acceptable restriction in the dynamic behavior for quick changes of radiation. Here, greater deviations caused by the thermal collector capacity occur. In contrast, the electrical power is much less sensitive to the ambient conditions and shows a good dynamic behavior. The influence of the cell temperature on the electrical power is usually by 4% per 10 K so that the power is primarily dependent on the radiation. Fig. 4.1 shows a systematic deviation between measured and simulated electrical power, which is the highest at the middle of the day. This indicates a systematic measurement error, which may be caused by the MPP tracker. In addition to that, the model was parameterized with the PV module datasheet and not with the measured electrical properties of the PV module in use.

4.3. Validation on pilot plant measurements

The PVT collector model is validated against measurements on a 40 m² PVT collector field. The collector field is integrated in a heat pump system with borehole heat exchanger and consists of 20 m² insulated and 20 m² not insulated PVT collectors of the same type. Insulated means in this case, that the back side of the PVT collector is equipped with an additional 3 cm thick mineral wool layer under the fluid system.

For the validation measurement data were used for the period of one year with the data of global and infrared radiation in collector area, air speed, the temperatures of ambient air and collector in- and outlet, fluid mass flow, electrical voltage and current and operating condition of the electrical inverter. For the electrical validation only daily periods were used, where array shading and low inverter power (less than 10% of rated power) could be excluded. The thermal validation includes all measured data. The measured yields in the period of one year was for the thermal yield 439.8 kWh/m² and for the electrical yield 74.3 kWh/m² (not insulated) and 74.4 kWh/m² (insulated). The uncertainty of the measurement for thermal yield has been determined to ±4.1% and for electrical yield to ±1.6% for the not insulated and ±1.7% for the insulated PVT collector field.

The diffuse radiation on collector surface was calculated with the Perez model in the TRNSYS type 16. The simulation time step was 1 minute equal to the interval of the averaged measured data. Fig. 4.2 displays the simulated and measured daily yields from April 2009 to March 2010. The deviation in the yearly thermal yield is +1.7% and for the relative square deviation 6.3%. For the electrical yield the deviation is +1.0% for

the insulated and +1.4% for the not insulated PVT collector field. The relative square deviation of the electrical yield is 2.7% for the insulated and 3.4% for the not insulated PVT collector field.

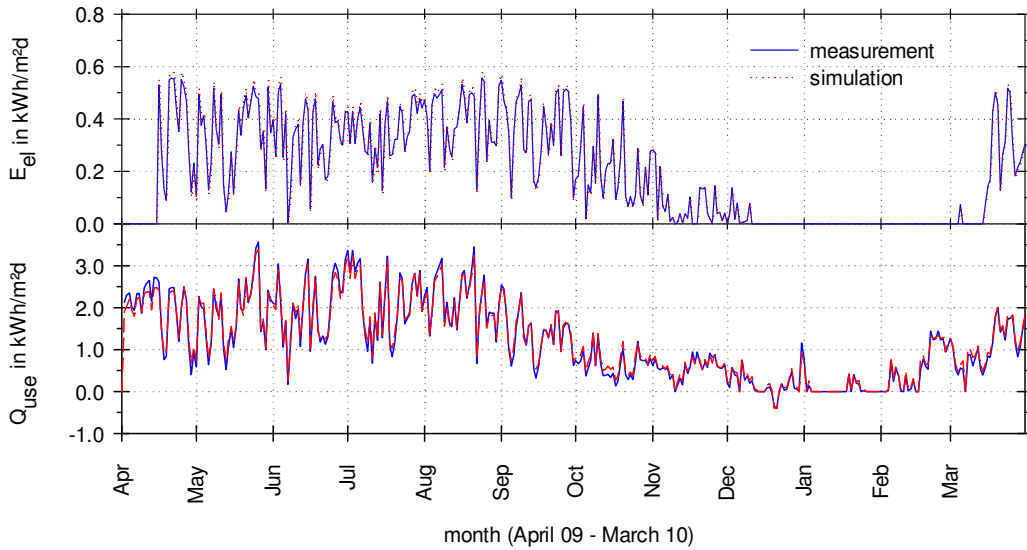


Fig. 4.2: Daily measured and simulated thermal and electrical yield of the pilot plant over the period of one year

In addition to that fig. 4.3 displays the monthly simulated and measured thermal and electrical yields over the same period. A good accordance between monthly simulated and measured yields may be seen, so that the developed model allows the simulation of thermal and electrical yield with high accuracy, for monthly and yearly periods.

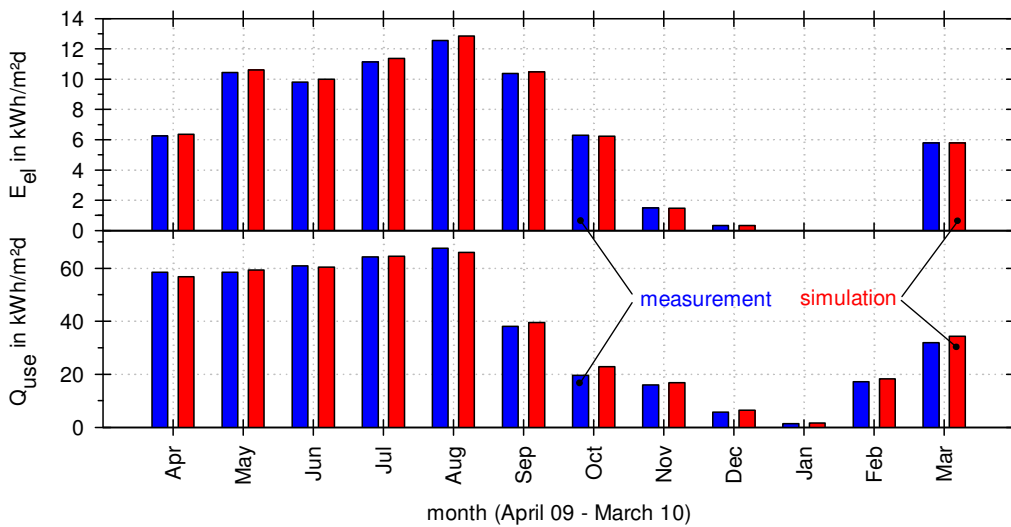


Fig. 4.3: Monthly measured and simulated thermal and electrical yield of the pilot plant over the period of one year

5. Conclusion

A new model for liquid cooled unglazed PVT collectors is presented, that combines the characteristic thermal and electrical performance models. The model was implemented in the simulation program TRNSYS. In contrast to existing models the new model requires only standard performance data, which are determined according to EN 12975-2 and EN 60904-1. The model includes the effects of air speed dependency, long-wave radiation to sky, thermal collector capacity and condensation effects on collector surface. Furthermore, the model was extended by an approach to determine the PV cell and module surface temperature. Therefore the internal heat transfer coefficient between PV cells and fluid is used. A method to calculate this internal heat transfer coefficient from the standard thermal performance data is proposed. The model was tested on test rig measurements and validated against a measurement of a pilot system over a

period of one year. The following table displays the validation results. The deviations between simulated and measured thermal and electrical yield values are given as relative deviations of total yields and as relative square deviations (see chapter 4.1).

Tab. 1: Deviations of simulated and measured thermal and electrical yields (relative deviation and relative square deviation)

	Thermal Yield		Electrical Yield			
			insulated		not insulated	
Measurement data from	ΔQ	\bar{V}	ΔE	\bar{V}	ΔE	\bar{V}
pilot plant	+1.7%	6.3%	+1.0%	2.7%	+1.4%	3.4%

It may be concluded, that the new model for unglazed PVT collectors allows the simulation of thermal and electrical yield with a high accuracy, if applied in long-term (e.g. monthly or annual) simulations. Only simulations with a high resolution of time and in cases of highly dynamic changes of input values values lead to significant differences. This model allows the evaluation of the electrical yield influenced by the cooling effect in comparison to a standard PV module.

6. Nomenclature

Symbol	Quantity	Unit
A	Area	m^2
b_1	Heat loss factor of PVT-collector	$W m^{-2} K^{-1}$
b_2	Air speed dependent heat loss factor	$J m^{-3} K^{-1}$
b_u	Air speed dependent conversion factor	$s m^{-1}$
c_L	Specific heat capacity of ambient air	$kJ kg^{-1} K^{-1}$
c_T	Temperature coefficient for electrical power of PV-module	$\% K^{-1}$
d	Diameter	m
Δh_v	Evaporation of water	$kJ kg^{-1}$
I	Current	A
k_{dif}	Incident angle correction factor for diffuse radiation	-
$k_{\theta, beam}$	Incident angle correction factor for beam radiation	-
Le	Lewis number ($Le = 0.87$ for water vapour in air)	-
\dot{m}	mass flow rate	$kg h^{-1}$
p_0	Air pressure	$mbar$
p_s	Water vapour saturation pressure	$mbar$
R_D	Gas constant of water ($R_D = 0.4614 kJ kg^{-1} K^{-1}$)	$kJ kg^{-1} K^{-1}$
R_L	Gas constant of air ($R_L = 0.2871 kJ kg^{-1} K^{-1}$)	$kJ kg^{-1} K^{-1}$
u	air speed	$m s^{-1}$
u_{loss}	heat loss coefficient	$W m^{-2} K^{-1}$
α	absorption coefficient	-
ε	emission coefficient	-
θ	Incident angle	$^\circ$
σ	Stefan Boltzmann constant ($5.67 \cdot 10^{-8} W m^{-2} K^{-4}$)	$W m^{-2} K^{-4}$

subscripts

amb	Ambient	$loss$	losses
$beam$	Beam	OC	Open circuit
DC	Direct current	out	outlet
dif	Diffuse	SC	Short circuit
in	Inlet	sky	Sky
l	Longitudinal	t	transverse

7. References

Balenzategui, J.L., Chenlo, F., 2005. Measurement and analysis of angular response of bare and encapsulated silicon solar cells. *Solar Energy Materials & Solar Cells* Volume 86 Issue 1.

Bertram, E., et al., 2009. Soil regeneration by unglazed solar collectors in heat pump systems. In *ISES Solar World Congress 2009 renewable energy shaping our future*. Johannesburg, South Africa: International Solar Energy Society.

- Duffie, J.A. & Beckman, W.A., 2006. *Solar Engineering of Thermal Processes* 3rd Aufl., Wiley.
- EN 12975-2 DIN Deutsches Institut für Normung e.V., 2006. Thermische Solaranlagen und ihre Bauteile, Kollektoren, Teil 2: Prüfverfahren, Deutsche Fassung EN 12975-2:2006, Beuth Verlag, Berlin.
- EN 60904-1 DIN Deutsches Institut für Normung e.V., 2007. Photovoltaische Einrichtungen - Teil 1: Messen der photovoltaischen Strom/Spannungskennlinien (IEC 60904-1:2006); Deutsche Fassung EN 60904-1:2006, Beuth Verlag, Berlin.
- Hilmer, F., et al., 1999. Numerical solution and validation of a dynamic model of solar collectors working with varying fluid flow rate. *Solar Energy* Vol. 65, No. 5.
- Rockendorf, G., et al., 1995. Methods to determine the internal heat transfer coefficient between absorber and fluid of solar collectors. In *Proceedings*. Solar World Congress ISES. International Solar Energy Society.
- Wagner, A., 2006. Photovoltaik Engineering, Handbuch für Planung, Entwicklung und Anwendung, 2., überarbeitete Auflage, Springer Verlag.